ELSEVIER

MD-simulation study of the hydrophobic hydration of nonionic surfactants

Dietmar Paschek [a], Thomas Engels [b], Alfons Geiger [a,*],
Wolfgang von Rybinski [b]

[a] *Physikalische Chemie, Universität Dortmund, 44221 Dortmund Germany*
[b] *Henkel KGaA, 40191 Düsseldorf Germany*

Abstract

The hydrophobic hydration of nonionic surfactants of general structure $H(CH_2)_m(OCH_2CH_2)_nOH$ (abbreviated as C_mE_n) as well as their constituents, namely small alkane and ether molecules, in dilute aqueous solutions have been investigated. By an extensive series of classical molecular dynamics simulations the temperature dependent association of surfactant molecules and hydrophobic test-particles are studied. The simulations were performed at constant ambient pressure conditions and temperatures between 275 and 450 K. The hydrophobic interaction has been probed by Widom's particle insertion method. The temperature dependence of the association process can be described well by temperature independent enthalpies and entropies of transfer of the test particle from bulk to shell. These transfer properties can be reduced to group contributions. The resulting Gibbs free energy of transfer was used as a measure of the hydrophobicity and could be correlated with the experimental cloud point temperatures of binary aqueous mixtures of these surfactants. An empirical correction leads to a quantitative description of the experimental data. © 1999 Elsevier Science B.V. All rights reserved.

Keywords: Molecular dynamics; Nonionic surfactants; Cloud point; Hydrophobic interaction

1. Introduction

Nonionic surfactants of the alkylpolyglycol ether type are key ingredients of detergent formulations because of their good detergency performance [1]. The interfacial and colloidal properties of alkylpolyglycol ethers have been the subject of numerous publications. In particular, the phase behavior of binary mixtures of water and nonionic surfactants has been studied intensively [2,3].

The phase behavior of nonionic surfactants with a low degree of ethoxylation is very complex. (see Fig. 1 for the lauryl-triglycol ether $C_{12}E_3$, as reproduced from [3]). In such systems at low surfactant concentrations an increase in temperature induces the transition from the isotropic L_1 single-phase into a two-phase system with two

* Corresponding author. Tel.: + 49-231-755-3937; fax: + 49-231-755-3937.
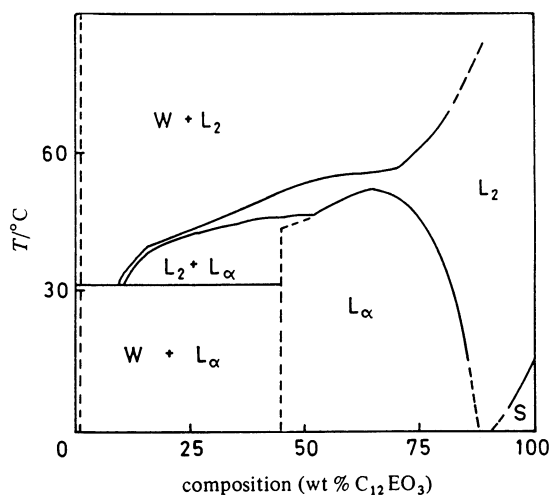*E-mail address:* geiger@pc2a.chemie.uni-dortmund.de (A. Geiger)

Fig. 1. Phase diagram of the $C_{12}E_3$ system. L_α, lamellar phase; L_2, liquid surfactant containing dissolved water; S, solid surfactant (reproduced from [3]).

coexisting liquid phases $(W + L_1)$. Since the transition is accompanied by a change from a transparent isotropic monomer or micellar solution into a turbid two-phase system it is usually called a 'cloudpoint'. This phase transition is a conse-

quence of a solubility decrease of the nonionic surfactant molecule with increasing temperature. The lower boundary curve of the two-phase region is shifted to lower temperatures with decreasing number of ethylene oxide units in the nonionic surfactant molecule.

Similar phenomena, which are based on the same physical principles, occur in three-phase systems consisting of oil, water and nonionic surfactant. During the phase transition usually very low interfacial tensions between the water and the oil phase are present. Because the interfacial tension is the restraining force with respect to the removal of liquid soils in washing and cleaning processes, systems with very low interfacial tensions should exhibit an optimal detergency performance. Fig. 2 (reproduced from [4]) shows for ternary systems of water alkylpolyglycol ether and alkane that the maximum of oil removal (e.g. for *n*-hexadecane, $n = 16$) is located in the three-phase interval (dotted area in Fig. 2b, [4,5]).

It was the purpose of this investigation to study the temperature dependent interaction of a single nonionic surfactant molecule of the alkylpolyglycol ether type with water and with hydrophobic
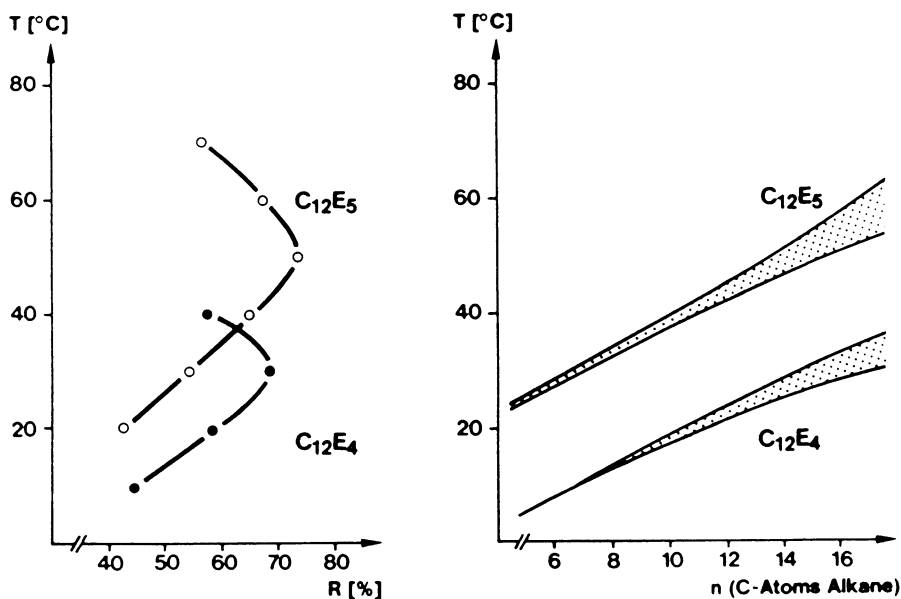

Fig. 2. Phase behavior and detergency of the polyoxyethylene alcohols $C_{12}E_4$ and $C_{12}E_5$ (reproduced from [4]): Three-phase temperatures vs number of carbon atoms *n* (right) and detergency *R* as a function of temperature (left).

test particles, using molecular dynamics computer simulations. The hydrophobic interaction with the test particle is quantified by the average chemical potential of this particle in the hydration shell of the surfactant molecule. This value is then used as a quantitative measure of the hydrophobicity of the solute. The hydrophobicity of the nonionic monomer is expected to change with temperature and its chemical composition. This should have an influence on the phase behavior of the system and therefore on the performance properties of the surfactant system.

Here three different nonionic surfactant molecules ($C_{12}E_3$, $C_{12}E_6$, C_8E_6) are considered in aqueous solution to study the effect of varying chain length of both ether- and alkyl-group. Additionally, an isolated ether chain $CH_3(OCH_2$-$CH_2)_2OCH_3$ (abbreviated as EO_3) surrounded by water is studied and an isolated alkane chain (n-hexane). From this limited number of simulations, which are based on the same set of interaction parameters, we are able to predict quantitatively the cloud point temperatures of a wide range of nonionic surfactants $H(CH_2)_m(OCH_2$-$CH_2)_nOH$ (abbreviated as C_mE_n), introducing in a final step a single adjustable parameter (called stabilisation entropy).

2. MD-simulations

2.1. Simulation techniques

All MD simulations were performed with the MOSCITO simulation package [6] employing a standard Verlet leap-frog integration scheme [7] in combination with SHAKE [8] to constrain fixed bond lengths. Cubic periodic boundary conditions and time-steps of 2 fs were used. The simulations were performed in the NPT-ensemble by applying the Berendsen weak coupling procedure [9] with temperature and pressure relaxation times of $\tau_T = 0.5$ ps and $\tau_p = 1.7$ ps (for the latter value a constant isothermal compressibility of 4.59 bar^{-1} has been assumed). To handle long range electrostatic forces and energies the smooth particle mesh Ewald (SPME) method of Essmann et. al. [10] was used with mesh spacings of about 1 Å,

B–H spline interpolation of 4'th order and an Ewald screening parameter of $\alpha = 2.98$ nm^{-1}. The real space part of the Ewald expression for the Coulomb interaction as well as the Lennard–Jones interactions were truncated at cutoff-distances of 9 Å. Lennard–Jones cutoff-corrections for potential energy and virial were adequately considered. The pressure evaluation has been performed by using a center of mass representation of the virial, described in Refs. [11,12].

2.2. Interaction models for solute and solvent

SPC/E [13] is used as a solvent model, since it has been shown that it reproduces the structural and thermodynamical properties of real water in the temperature regime above 270 K rather well [14–16]. Moreover, the location of the liquid–gas critical point being only about 7 K below the value for real water [15] is an astonishing coincidence for a model which has been parametrised originally for ambient temperature conditions. As it has been pointed out by Guillot and Guissani [14] the model gives an almost quantitative description of rare gas solubilities in water over the wide temperature range from 270 to 650 K. Therefore, it seems well suited as solvent model to study the temperature dependence of hydrophobic interactions of non-polar and weakly polar particles in water.

For the description of the solute molecules elements of different force-fields were used. For the ether component a model originally derived for poly-oxy-ethylene (POE) by Müller-Plathe [17] was used, where the torsion potentials were refined according to the ab initio data of Gejji et al. [18]. For the OH-group the original OPLS-Parameters of Ref. [19] were employed, combined with a refined ab initio torsion potential explicitly derived for β-oxy-hydroxyl groups. Two different approaches were discussed for the description of the alkyl-groups: for the united atom representation the modified OPLS-model parametrisation of Smit et al. [20] was used with zero charges on all alkane-sites. Additionally, an all atom representation of the alkyl-chain was studied by the use of the Cornell et al. forcefield [21] in combination with the charge model described in Ref. [22].

Lennard–Jones cross terms were determined by Lorentz–Berthelot combination rules. All bond-lengths were kept fixed during the simulation runs. In summary, for the solute molecules a combination of several popular force-fields was used. The parameters can be found in the references given above, with the exception of some torsion potentials, which were refined by the use of ab initio data. A detailed description of the analytical form of the interaction potentials and a compilation of all employed parameters are also given in [23]. It should be stressed here, that the interaction potential is the most crucial and important input to a simulation. The predictive power of a simulation depends strongly on the care which has been spent on the development of the force-field prior to the simulation. Furthermore, it is emphasised, that once the force-field had been chosen in this initial step, this was not subjected to any more fitting procedure to adjust the simulation results.

2.3. MD-outline

Initially, a single solute molecule is placed in the center of a cubic water system with a density of 1.0 g cm^{-3} removing all overlapping water molecules. Depending on the size of the solute, the system sizes were chosen sufficiently large to guarantee the absence of an interaction of the solute molecule with the hydration shell of its own image (see Table 1). These systems were simulated at the chosen state-points (275, 300, 325, 350, 375, 400 and 450 K) for an equilibration period of 0.1–0.5 ns (50 000–250 000 timesteps). The subsequent production runs extended to time intervals given in Tables 1 and 2. Approximately 5000 configurations, equally spaced over the whole simulation run, were examined at each state-point. The location of the studied state-points compares rather well with previously published data [14,16,24].

3. Test particle method and quantified hydrophic interaction (QHI) model

The present study is aimed to determine the

Table 1
Outline of solute/solvent systems studied here[a]

Solute molecule	No. solvent molecules	Production run lengths (ns)
n-Hexane (all-atom model)	319	1.8–2.0
n-Hexane (united-atom model)	329	2.0
EO$_3$	314	2.0
C$_{12}$E$_6$	1309	1.0–2.0
C$_{12}$E$_3$	688	1.1
C$_8$E$_6$	1315	1.0–1.3
Pure SPC/E	256	2.0

[a] For each system seven different state-points were considered (275, 300, 325, 350, 375, 400 and 450 K). All systems had been equilibrated before in explicit equilibration runs of 0.1–0.5 ns length.

temperature dependence of the hydrophobic interaction of nonionic surfactants. For this purpose the solvent induced interaction of a hydrophobic test particle with nonionic surfactant molecules as a whole and with particular parts (groups) of the

Table 2
Thermodynamic data characterising the examined state-points of the dilute aqueous systems. The data shown here were obtained from the production runs of the pure water phase[a]

T (K)	ρ (g cm^{-3})	*p* (MPa)	$E_{pot.}$ (kJ mol^{-1})
274.6 ± 0.8	1.0085 ± 0.0018	−0.6 ± 5.0	−48.48 ± 0.05
299.6 ± 0.7	0.9990 ± 0.0017	−0.6 ± 7.9	−46.88 ± 0.05
324.6 ± 0.9	0.9846 ± 0.0015	−0.2 ± 7.1	−45.38 ± 0.04
349.8 ± 0.9	0.9673 ± 0.0015	−3.1 ± 6.5	−43.90 ± 0.03
374.4 ± 0.8	0.9468 ± 0.0010	0.0 ± 5.7	−42.44 ± 0.03
399.9 ± 1.7	0.9231 ± 0.0011	−1.0 ± 10.5	−41.03 ± 0.04
449.9 ± 1.0	0.8676 ± 0.0011	1.6 ± 5.2	−38.12 ± 0.04

[a] The errors were determined as proposed in Ref. [7].

molecule was studied. Since this type of interaction has to be determined as a free energy difference, the Widom test particle method [25] was applied as an efficient way to evaluate absolute free energies and free energy differences from the simulation trajectories.

In the canonic ensemble the excess chemical potential μ_{ex} (the solvation free energy of a solute particle $(N+1)$ in a N particle solvent) is given by

$$\mu_{\text{ex}} = \Delta F = -\beta^{-1} \frac{Z_{\beta,N+1}}{V Z_{\beta,N}}, \qquad (1)$$

where $\beta = 1/k_{\text{B}}T$ is the inverse temperature, V the volume and $Z_{\beta,N}$ the configurational partition function of the N particle system at T and V

$$Z_{\beta,N} = V^N \int \exp(-\beta U(s_1 \ldots s_N, L)) \, ds_1 \ldots ds_N. \quad (2)$$

$U(s_1 \ldots s_N, L)$ is the potential energy of the N-particle system. s_N are scaled coordinates of the particles with $s_N = r_N/L$, where L is the box-length of the cubic system. Particle $N+1$ is the inserted test particle. As pointed out by Widom already in the 1960s [26], Eq. (1) can be rewritten to

$$\mu_{\text{ex}} = -\beta^{-1} \int \langle \exp(-\beta \phi(s_{N+1}, L)) \rangle_N \, ds_{N+1} \tag{3}$$

which makes it possible to determine the excess chemical potential as a conventional thermodynamic average of a quantity $\exp(-\beta\phi)$. Here $\langle \ldots \rangle_N$ denotes ensemble averaging over the configurational space of the N-particle system and ϕ is the potential energy of particle $(N+1)$ inserted into the system of N solvent molecules at position s_{N+1}. The pair correlation function of the inserted solute particle with respect to selected reference sites in the simulated system (N_{Ref} is the number of equivalent reference sites) can be determined as

$$g(r) = \frac{1}{N_{\text{ref}}}$$

$$\frac{\int \left\langle \sum_{i=1}^{N_{\text{ref}}} \delta(|s_{N+1} \cdot L - r_i| - r) \exp[-\beta\phi] \right\rangle_N \, ds_{N+1}}{\int \langle \exp[-\beta\phi] \rangle_N \, ds_{N+1}}. \tag{4}$$
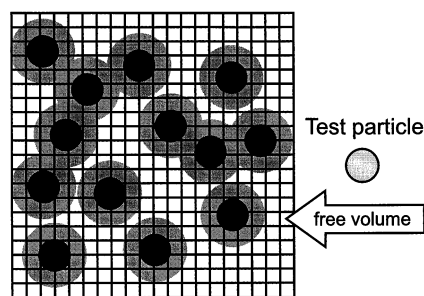

Fig. 3. Schematic illustration of the grid based excluded volume map. The grey regions represent the excluded volume of the black particles in the N-particle system. The radius of the excluded spheres is determined by the Lennard–Jones σ of the interaction with the test particle.

Although not rigorously correct for the NPT ensemble, application of Eq. (3) serves as a reasonable estimate for the excess chemical potential in the present study, since the effect of the volume fluctuations [25] was not found to affect the data significantly. Eq. (4) is related to the profile of free energy $w(r)$ (also referred to as potential of mean force (PMF)) for the association of the inserted test particle with selected reference sites [27] by

$$w(r) = -\beta^{-1} \ln g(r) + C. \tag{5}$$

where C is an undetermined integration constant which is of no importance here, since interest lies in free energy differences with respect to the same reference state. To speed up numerically the volume integration of Eq. (3), values for the potential energy were evaluated only for insertions in the free volume of a configuration. This has been determined by an excluded volume map, where the excluded volume is mapped on a grid with approximately 0.2 Å (exact values depend on the system size) mesh spacing. The excluded volume is defined by a distance less than 0.8σ between the grid point and any molecular site (σ is the Lennard–Jones parameter of the interaction between test particle and molecular site). Fig. 3 illustrates this particle insertion method. In the preliminary trial runs this procedure has been found to affect the obtained chemical potential by less than 0.02 kJ mol^{-1} over the considered temperature range. To ensure a comparable statistics of the test particle chemical potential in the vicinity of the surfac-

tant molecules, for any system about 120 successful insertions ($\equiv$ insertions into the free volume) per nm³ and configuration were performed.

Besides computing the profile of free energy as a function of distance from particular sites, we consider the integral in the vicinity of a surfactant as a quantitative measure of 'hydrophobicity'. The construction of the solute volume (the integration volume) is indicated in Fig. 4. Around each non hydrogen center of the solute molecule a sphere of 0.65 nm radius is drawn. The solute volume belonging to a particular site is defined by its larger distance with respect to any other site. As also indicated in Fig. 4, the solute volume of different sites of the molecule can be added up to form a group. The described procedure ensures a strict additive partitioning of the entire solute volume. As standard test particle a Ne atom was used ($\sigma_{\text{Ne–Ne}} = 3.2$ Å, $\epsilon_{\text{Ne–Ne}}/k_B = 38.12$ K). The use of the rather small Ne-particle is highly advantageous since it guarantees a sufficiently large free volume fraction (about 2% in the water bulk with a tendency to increase slightly at higher temperatures) in order to ensure appropriate statistics for the obtained excess chemical potential values. Moreover, a variation of the test parti-
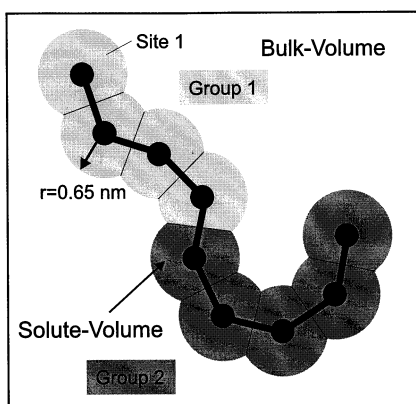

Fig. 4. Illustration of the quantified hydrophic interaction (QHI) solute volume partitioning. Around each non-hydrogen center of the solute molecule a sphere of 0.65 nm radius is drawn. The solute volume of a particular site is defined by all points which have a larger distance to any other site. Sites belonging to particular parts of the molecule (e.g. alkyl-chain) can be combined to form a group solute volume.

cle type should not affect the temperature dependence of the hydrophobic interaction dramatically since the excess chemical potential of particles of different size is more or less shifted by a constant value [14,28]. Values of the excess chemical potential are referred to for the standard Ne obtained from the outlined solute volume as QHI model data.

4. Discussion

4.1. Profile of free energy

In this section the temperature dependence of the hydrophobic association between the chosen standard hydrophobic particle and the two constituent groups of the surfactants is discussed. For this purpose the ether molecule EO₃ and the two different models chosen for *n*-hexane are considered (see Table 1). In Fig. 5 the profile of free energy for the association of a Ne particle and characteristic solute molecule centers at infinite dilution are shown. Two main features are observed: first, with increasing temperature the hydrophobic interaction becomes increasingly attractive for both ether and alkane group. This general feature is in accordance with previous findings for pairs of Lennard–Jones solutes [29–34]. Note the absence of any convergence of the well depths at high temperature as it was found in the work of Lüdemann et al. [32,33] for pairs of methane-like particles. This difference may be attributed to the fact that Lüdemann et al. studied constant volume conditions, whereas here the density effect was taken into account. Secondly, comparing Fig. 5a,b with Fig. 5c,d, a stronger temperature behavior of the PMF can be denoted with respect to the alkane group than for the ether group sites. The temperature dependence within the considered temperature range can be reasonably described by a division into temperature independent entropic and enthalpic contributions according to

$$w(r) = h(r) - Ts(r). \tag{6}$$

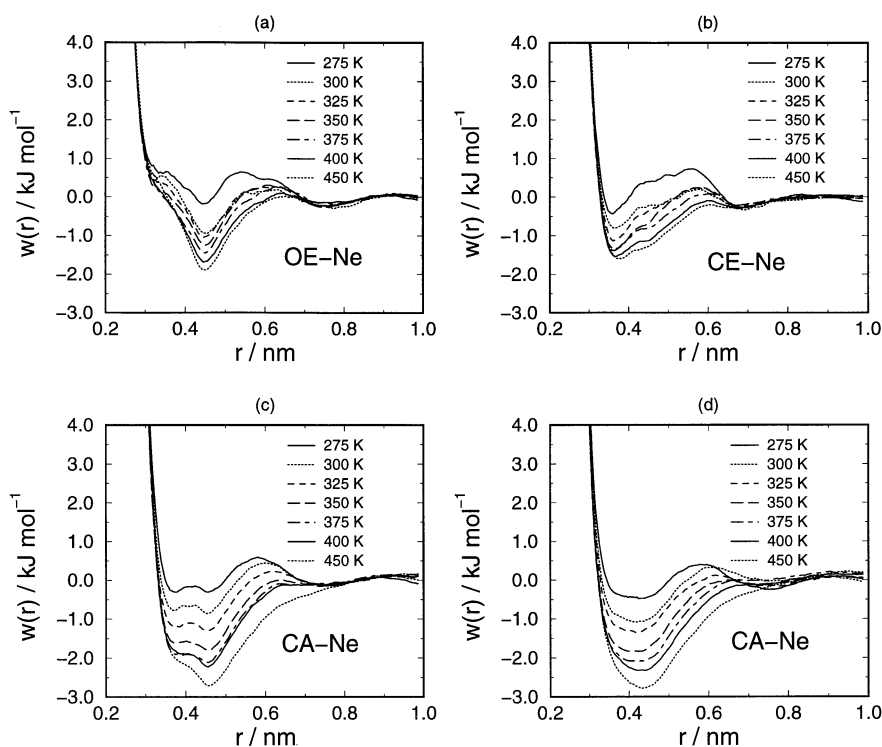The enthalpic and entropic parts shown in Fig. 6 were obtained by fitting Eq. (6) to the data

Fig. 5. Profiles of free energy $w(r)$ for the association of a Ne test-particle with particular sites of selected solute molecules at infinite dilution. (a) Ether-oxygen in EO_3. (b) Ether-carbon in EO_3. (c) Alkyl-carbon in *n*-hexane (all atom model). (d) Alkyl-carbon in *n*-hexane (united atom model).

depicted in Fig. 5. As can be seen clearly, the temperature dependence can be understood as a consequence of compensating large repulsive enthalpic and attractive entropic contributions. As it has been conjectured from Fig. 5, both terms are systematically more pronounced for the alkane chain sites. To support the procedure given above, it is shown in Fig. 7 $w(r)$'s synthesised according to Eq. (6), which compare well with the original PMF data obtained from particle insertion in Fig. 5d. An interesting side-aspect of the work presented here is a comparison of interaction models of different type, namely the all atom and united atom models for *n*-hexane. Comparing Fig. 5c and d, it has to be denoted that the all atom model exhibits the existence of a double minimum structure of the potential well, whereas the united atom model shows only one broad minimum. Despite this

difference, the temperature effects for both groups seem to coincide rather well, which becomes even more clearly evident from Fig. 6. From this data as well as solute–water pair correlation functions (not shown here) it turns out that the structural differences have to be attributed to slightly different structural packing of water molecules around the less isotropically interacting all atom carbon centers. However, the water–water structure and consequently the temperature dependence of the hydrophobic interaction does not seem to be strongly influenced by the actual model chosen. To summarise, it can be concluded that one of the main features of Figs. 5 and 6 is the connection of hydrophobic interaction strength with the polarity of the actual solute molecule and the possibility to extract this information from a series of MD-simulations. In the next section this rela-
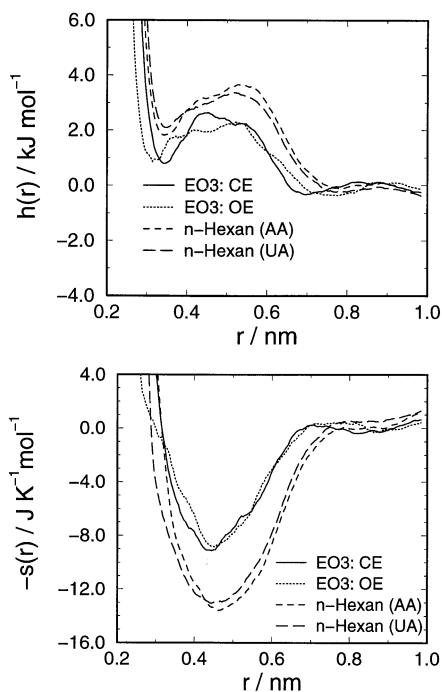
Fig. 6. Temperature independent enthalpic and entropic contributions (Eq. (6)) to the profiles of free energy of Fig. 5.

tion will be evaluated more quantitatively and it will show a strong correlation with the position of the experimental cloud points.
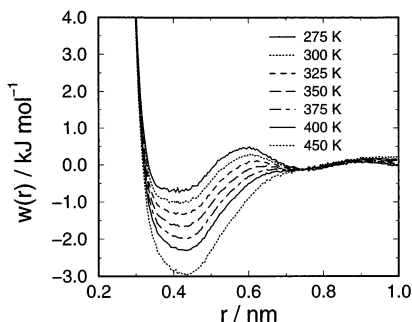

Fig. 7. Profiles of free energy $w(r)$ for the association of a Ne test-particle with the carbon sites in *n*-hexane (united atom model) constructed according to Eq. (6) from the data shown in Fig. 6. These have to be compared with the original simulation data given in Fig. 5d.
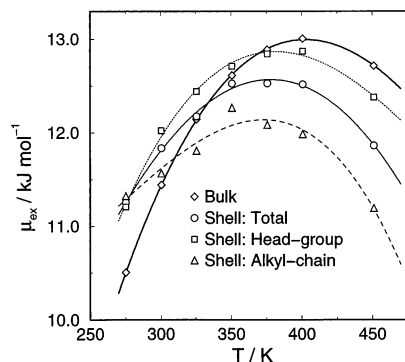

Fig. 8. Comparison of the excess chemical potential of a Ne particle in the bulk phase with values obtained for the shell of the surfactant $C_{12}E_6$. Note the different temperature behavior of head-group (ether-chain plus OH-group) and alkyl-chain. The lines represent fits of the data to polynomials of cubic order.

4.2. QHI model and experimental cloud points

In Fig. 8 the average chemical potential of the Ne particle in the bulk phase as well as in the shell volume of the surfactant $C_{12}E_6$ is shown as a function of temperature. There are two interesting features: first, an intersection of the temperature dependences in bulk and shell are observed. Moreover, for different parts of the shell (head-group and alkyl-chain) the intersection temperature is shifted significantly. A typical intersection temperature of about 320 K is found for the alkyl chain and 380 K for the head group, independent of the specific surfactant solute molecule.
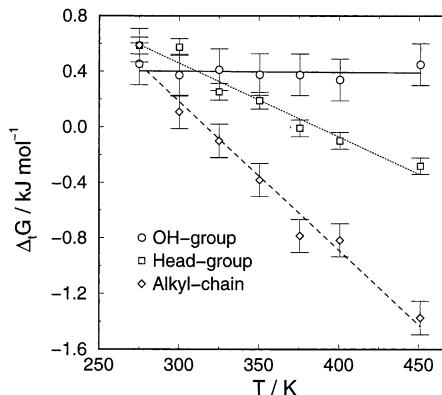

Fig. 9. Average free energy of transferring a Ne particle from bulk to shell for several groups of the studied surfactants.

In Fig. 9 the differences between the chemical potentials of Ne in shell and bulk, denoted as free energy of transfer from bulk to shell

$$\Delta_t G = \mu_{ex}(\text{Shell}) - \mu_{ex}(\text{Bulk}), \tag{7}$$

are shown. To obtain these values, the group contributions are averaged over all solute molecules from the simulations. The error bars result from this averaging procedure. As already demonstrated before for the profile of free energy, Fig. 9 is indicating that the free energy of transferring a hydrophobic particle from the bulk to the solvation shell is a linear function of temperature. Therefore, a division into temperature independent enthalpic and entropic terms according to

$$\Delta_t G = \Delta_t H - T \Delta_t S \tag{8}$$

is reasonable. It becomes evident from Fig. 9 that the polarity of a group controls the temperature dependence of the association with a hydrophobic particle. In other words, the transfer-entropy of an apolar test particle from bulk to shell depends strongly on the polarity of the group considered.

From the point of view of the hydrophobic test particle this can be understood by different temperature dependences of the water structure in the shell volume with respect to the bulk phase. In the vicinity of an OH-group the water structure is very similar to the bulk phase since the OH-group is involved into the hydrogen bond network. Therefore, no significant temperature dependence is observed. The opposite situation is found for the hydration shell of an apolar alkane-chain. There is evidence from analysing structural and energetic properties of the shell water (not shown here and discussed in detail in a forthcoming publication) that it behaves similar to water under tension [35].

In addition to the previous observations it is found that the average excess chemical potential for the total surfactant solvation shell can be expressed as weighted sum of the group contributions. Moreover, the shell volumes attributed to the groups are rather well linearly related to the stoichiometric coefficients m and n. Assuming temperature independent enthalpies and entropies as indicated by the QHI-data the observed group additivity suggests to predict the intersection tem-

Table 3
Thermodynamic parameters determining the transfer free energy for head-group and alkane-chain over the studied temperature range

Head-group	Alkane-chain
$\Delta_t H^E = 2100 \text{ J mol}^{-1}$	$\Delta_t H^C = 3400 \text{ J mol}^{-1}$
$\Delta_t S^E = 5.3 \text{ J K}^{-1} \text{ mol}^{-1}$	$\Delta_t S^C = 10.7 \text{ J K}^{-1}$ mol^{-1}

perature (where $\Delta_t G = 0$) for the entire molecule from the transfer properties of the different groups depending on the chemical composition according to

$$T_s = \frac{\Delta_t H}{\Delta_t S}, \tag{9}$$

with

$$\Delta_t H = (1 - \lambda) \Delta_t H^E + \lambda \Delta_t H^C$$
$$\Delta_t S = (1 - \lambda) \Delta_t S^E + \lambda \Delta_t S^C, \tag{10}$$

where λ is the fraction of the hydration shell volumes of head-group and alkane-chain (superscripts E and C). It is found that λ can be expressed by the stoichiometric coefficients m and n

$$\lambda = \frac{m}{m + fn}, \tag{11}$$

where f takes account of the actual size of the constituent groups. f was found to be 2.9 (The ether group units are about three times as big as the methylen groups). The values which were obtained by fitting Eqs. (8), (10) and (11) to the data of Fig. 9, are given in Table 3. With these parameters, obtained from the simulations of three specific surfactant molecules, the intersection temperature T_s can now be predicted for any given surfactant molecule $C_m E_n$.

In the last part of this contribution we try to relate the predicted intersection temperature T_s, which is a purely molecular property, with macroscopic properties like the position of the lower critical solution temperature of aqueous surfactant mixtures or experimental cloud point temperatures. This approach is motivated by the fact that the location of the critical point of a van der

Waals gas is determined by its mean field interaction parameters. However, in the present case not much is known about such interaction parameters, nor about the structure of an appropriate equation of state. Nevertheless, neglecting any further structural aspects of the complex aqueous surfactant mixtures and starting from the MD-simulation results, it is conjectured that the location of the intersection temperature T_s might be related to the lower critical solution temperature. A rather heuristic argument for such an expectation is the fact, that the transfer free energy of the hydrophobic test particle changes its sign at T_s, indicating an increasing tendency for aggregation with increasing temperature.

A comparison of the determined intersection temperatures with a large set of experimental cloud point temperatures [36,37] shows that the values are well correlated (see Fig. 10). However, the data do not coincide perfectly since the hydrophobic test particle employed is only a very rough

Fig. 11. Correlation of the empirically corrected intersection temperatures T_s with experimentally obtained cloud point temperatures T_c.

estimate for the chemical potential of a complete surfactant molecule in a micellar solution. Nevertheless, as also indicated by Fig. 10, there is a far better correlation with the cloud point data when considering constant ether or alkane chain lengths. Here it should be stressed once more that up to this point no fitting to any experimental data has been done, only molecular dynamics simulations of dilute aqueous solutions with conventional force fields have been used. To take the apparently important chain length effect into account, an empirical term is now introduced, the so called stabilisation entropy $\Delta_{stab}S$ and replace in Eq. (9) $\Delta_t S$ by $\Delta_t S'$

$$\Delta_t S' = \Delta_t S + \Delta_{stab}S. \tag{12}$$

$\Delta_{stab}S$ is estimated to be linearly dependent on the size of the surfactant groups with

$$\Delta_{stab}S = m\Delta_{stab}S^C + n\Delta_{stab}S^E. \tag{13}$$

The values were determined empirically for optimum correlation to $\Delta_{stab}S^C = -0.024$ J K^{-1} mol^{-1} and $\Delta_{stab}S^E = 0.025$ J K^{-1} mol^{-1}. The corresponding values for T_s', shown in Fig. 11, allow a quantitative prediction of the cloud point temperatures based on the given values, when using the scaling relation

$$T_c = (T_s' - T_s^0)k_s, \tag{14}$$

with the parameters $k_s = 0.1324$ and $T_s^0 = 314.3$ K. In Table 4 a comparison between these data and the experimental cloud point temperatures [36,37] are given.
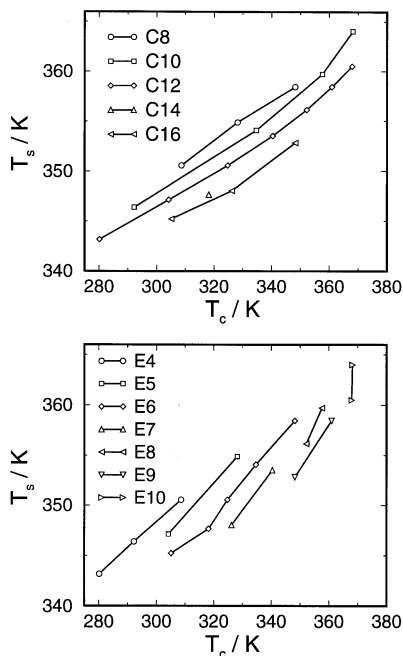

Fig. 10. Correlation between intersection temperatures T_s and experimental cloud point temperatures T_c as a function of alkane chain length (upper diagram) and ether-chain length (lower diagram).
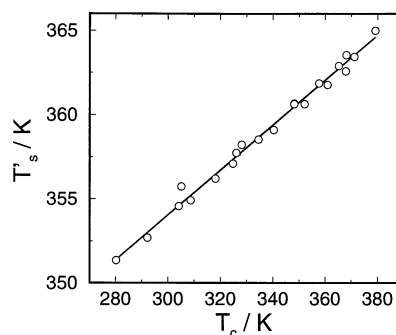
Table 4
Comparison of experimental cloud point temperatures [36, 37] with values obtained from the quantified hydrophic interaction (QHI) data approach with entropy correction term

M	n	T_c (°C) (expt.)	T_c (°C)	ΔT_c (°C)
8	4	35.5	33.4	−2.1
8	5	55.0	58.3	3.3
8	6	75.0	76.5	1.5
8	12	106.0	109.2	3.2
10	4	19.0	16.7	−2.1
10	6	61.5	60.6	−0.9
10	8	84.5	85.5	1.1
10	10	95.0	98.2	3.2
12	4	7.0	6.8	−0.2
12	5	31.0	30.9	−0.1
12	6	51.6	50.0	−1.6
12	7	67.2	64.9	−2.3
12	8	79.0	76.3	−2.7
12	9	87.8	84.9	−2.9
12	10	94.8	91.0	−3.8
12	12	98.0	97.4	−0.6
14	6	45.0	43.3	−1.7
16	6	32.0	39.7	7.7
16	7	53.0	54.7	1.7
16	9	75.0	76.4	1.4
16	12	92.0	93.2	1.2

5. Conclusions

The hydrophobic hydration of nonionic akylpolyglycol ether type surfactant in dilute aqueous solutions, as well as their constituents. have been studied extensively by a series of classical molecular dynamics computer simulations. The calculations were done for constant ambient pressure conditions and fixed temperatures in a range between 275 and 450 K applying Widom's particle insertion method. The temperature dependent association of surfactant molecules and hydrophobic neon test particles can be described well by temperature independent enthalpies and entropies of transfer of the test particle from the bulk to the hydration shell of the surfactant. These transfer properties can be reduced to group contributions. The resulting Gibbs free energy has been taken as a measure of the hydrophobicity and can be correlated with experimental cloud point temperatures of binary aqueous mixtures of these nonionic surfactants. A term called stabilisation entropy is introduced in order to take into account that interacting groups are not independent, but attached to neighbors within the chains. This empirical correction finally enables a quantitative prediction of the experimental cloud point temperatures for any kind of alkylpolyglycol ether surfactant in water. This has important consequences for the performance evaluation of surfactants.

References

[1] H. Andree, P. Krings, Waschmittelchemie, Hüthig, Heidelberg, 1976, p. 84.
[2] J.C. Lang, R.D. Morgan, J. Chem. Phys. 73 (1980) 5849.
[3] D.J. Mitchell, G.J.T. Tiddy, L. Warring, T. Bostock, M.P. McDonald, J. Chem. Soc. Faraday Trans. I 79 (1983) 975.
[4] F. Schambil, M.J. Schwuger, Colloid Polymer Sci. 265 (1987) 1009.
[5] M. Kahlweit, R. Strey, in: H.L. Rosano Jr. (Ed.), Proceedings of the Vth International Conference on Surface and Colloid Science, Marcel Dekker, New York, 1985.
[6] D. Paschek, MOSCITO A free MD simulation package, Universität Dortmund, 1998, the software and user's guide are available through the internet following the URL: http://ganter.chemie.uni-dortmund.de/.
[7] M.P. Allen, D.J. Tildesley, Computer Simulation of Liquids, Oxford Science Publications, Oxford, 1989.
[8] J.P. Ryckaert, G. Ciccotti, H.J.C. Berendsen, J. Comp. Phys. 23 (1977) 327.
[9] H.J.C. Berendsen, J.P.M. Postma, W.F. van Gunsteren, A. DiNola, J.R. Haak, J. Chem. Phys. 81 (1984) 3684.
[10] U. Essmann, L. Perera, M.L. Berkowitz, T.A. Darden, H. Lee, L.G. Pedersen, J. Chem. Phys. 103 (1995) 8577.
[11] S. Nosé, M.L. Klein, Mol. Phys. 50 (1983) 1055.
[12] J. Alejandre, D.J. Tildesley, G. Chapela, J. Chem. Phys. 102 (1995) 4574.

[13] H.J.C. Berendsen, J.R. Grigera, T.P. Straatsma, J. Phys. Chem. 91 (1987) 6269.

[14] B. Guillot, Y. Guissani, J. Chem. Phys. 99 (1993) 8075.

[15] Y. Guissani, B. Guillot, J. Chem. Phys. 98 (1993) 8221.

[16] S. Harrington, P.H. Poole, F. Sciortino, H.E. Stanley, J. Chem. Phys. 107 (1997) 7443.

[17] F. Müller-Plathe, Acta Polymer. 45 (1994) 259.

[18] S.P. Gejji, J. Tegenfeldt, J. Lindgren, Chem. Phys. Lett. 226 (1994) 427.

[19] W.L. Jorgensen, J. Phys. Chem. 90 (1986) 1276.

[20] B. Smit, S. Karaborni, J.I. Siepmann, J. Chem. Phys. 102 (1995) 2126.

[21] W.D. Cornell, P. Cieplak, C.I. Bayly, I.R. Gould, K.M. Merz Jr., D.M. Ferguson, D.C. Spellmeyer, T. Fox, J.W. Caldwell, P.A. Kollman, J. Am. Chem. Soc. 117 (1995) 5179.

[22] W.L. Jorgensen, D.S. Maxwell, J. Tirado-Rives, J. Am. Chem. Soc. 118 (1996) 11225.

[23] D. Paschek, Molekulardynamik Simulation der hydrophoben Hydratation nichtionischer Tenside, Dissertation, Universität Dortmund, 1998.

[24] L.A. Baez, P. Clancy, J. Phys. Chem. 101 (1994) 9837.

[25] D. Frenkel, B. Smit, Understanding Molecular Simulation—From Algorithms to Applications, Academic Press, San Diego, 1996.

[26] B. Widom, J. Chem. Phys. 39 (1963) 2808.

[27] D.A. McQuarrie, Statistical Mechanics, Harper and Row, New York, 1973.

[28] S. Garde, G. Hummer, A.E. García, M.E. Paulaitis, L.R. Pratt, Phys. Rev. Lett. 77 (1996) 4966.

[29] D.E. Smith, L. Zhang, A.D.J. Haymet, J. Am. Chem. Soc. 114 (1992) 5875.

[30] D.E. Smith, A.D.J. Haymet, J. Chem. Phys. 98 (1993) 6445.

[31] J. Forsman, B. Jonsson, J. Chem. Phys. 101 (1994) 5116.

[32] S. Lüdemann, H. Schreiber, R. Abseher, O. Steinhauser, J. Chem. Phys. 104 (1996) 286.

[33] S. Lúdemann, R. Abseher, H. Schreiber, O. Steinhauser, Am. Chem. Soc. 119 (1997) 4206.

[34] S.W. Rick, B.J. Berne, J. Phys. Chem. B 101 (1997) 10488.

[35] A. Geiger, P. Mausbach, Hydrogen-Bonded Liquids, ASI, NATO, Kluwer, Netherlands, 1991, pp. 171–183.

[36] H. Lange, M.J. Schwnger, in: K. Henkel (Ed.), Fatty Alcohols—Raw Materials, Methods, Uses, vol. 1, Henkel KGaA, Dusseldorf, 1982, pp. 87–119.

[37] T. Engels (unpublished).